Photoluminescence and transport studies of boron in 4H SiC

S. G. Sridhara, L. L. Clemen, R. P. Devaty, W. J. Choyke, D. J. Larkin, H. S. Kong, T. Troffer, and G. Pensl

Citation: Journal of Applied Physics **83**, 7909 (1998); doi: 10.1063/1.367970
View online: http://dx.doi.org/10.1063/1.367970
View Table of Contents: http://scitation.aip.org/content/aip/journal/jap/83/12?ver=pdfcov
Published by the AIP Publishing

Photoluminescence and transport studies of boron in 4H SiC

S. G. Sridhara, L. L. Clemen, R. P. Devaty,[a] and W. J. Choyke
Department of Physics and Astronomy, University of Pittsburgh, Pittsburgh, Pennsylvania 15260

D. J. Larkin
NASA Lewis Research Center, MS 77-1, 21000 Brookpark Road, Cleveland, Ohio 44135

H. S. Kong
Cree Research, Inc., 2810 Meridian Parkway, Suite 176, Durham, North Carolina 27713

T. Troffer and G. Pensl
Lehrstuhl für Angewandte Physik, Universität Erlangen-Nürnberg, Staudtstr. 7, D-91058 Erlangen, Germany

(Received 2 February 1998; accepted for publication 23 March 1998)

Two distinct boron-related centers are known in silicon carbide polytypes, one shallow (ionization energy ~ 300 meV) and the other deep (~ 650 meV). In this work, 4H SiC homoepitaxial films are intentionally doped with the shallow boron center by controlling the silicon to carbon source gas ratio during chemical vapor deposition, based on site competition epitaxy. The dominance of the shallow boron center for samples grown with a low Si/C ratio, favoring the incorporation of boron onto the silicon sublattice, is verified by the temperature dependent Hall effect, admittance spectroscopy and deep level transient spectroscopy. In these samples a peak near 3838 Å appears in the low temperature photoluminescence spectrum. Further experiments support the identification of this peak with the recombination of a four particle (bound exciton) complex associated with the neutral shallow boron acceptor as follows: (1) The intensity of the 3838 Å peak grows with added boron. (2) Momentum conserving phonon replicas are observed, with energies consistent with other four particle complexes in SiC. (3) With increasing temperature excited states are observed, as for the neutral aluminum and gallium acceptor four particle complexes. However, the intensity of the shallow boron spectrum is quenched at lower temperatures than the corresponding spectra for Al and Ga, and the lineshapes are strongly sample dependent. These results may be related to the unusual configurational and electronic structure of this center inferred from recent spin resonance experiments by other groups. When the Si/C ratio is high, the optical signatures of the deep boron center, nitrogen-boron donor-acceptor pairs and conduction band to neutral acceptor free-to-bound transitions, are observed in the photoluminescence. At $T=2$ K well resolved, detailed nitrogen-boron pair line spectra are observed in addition to the peak due to distant pairs. As the temperature is raised, the donor-acceptor pair spectrum decreases in intensity while the free-to-bound no-phonon peak appears. Extrapolation of the temperature dependence of the free-to-bound peak to $T=0$ K, after correction for the temperature dependence of the exciton energy gap, leads to the value $E_A(B)-E_X=628\pm 1$ meV, where $E_A(B)$ is the ionization energy of the deep boron center and E_X is the binding energy of the free exciton which, for 4H SiC, can only be estimated at this time. © *1998 American Institute of Physics.* [S0021-8979(98)08212-7]

I. INTRODUCTION

Boron as an impurity in silicon carbide polytypes has been studied for over 40 years, but its behavior is not completely understood. It can act as a p-type dopant and participates in luminescence. Boron is a common unintentional contaminant in part due to its presence in graphite components of the growth apparatus.

A shallow boron acceptor level is measured by the temperature dependent Hall effect[1] and admittance spectroscopy.[2] In the case of 4H SiC, the subject of this article, the measured ionization energy is 285 ± 10 meV.[2] Electron spin resonance (ESR) and electron nuclear double resonance (ENDOR)[3–9] on 4H-, 6H-, and 3C-SiC indicate that this boron replaces Si and that the configuration, electronic structure, and temperature dependence do not support the model of a substitutional effective mass acceptor.

A deep boron level (ionization energy $\sim 0.6-0.7$ eV) participates in luminescence via nitrogen-boron donor acceptor pairs (DAP) at low temperatures and conduction band to neutral boron acceptor free to bound (FB) transitions when electrons are thermally excited into the conduction band. Yamada and Kuwabara[10] analyzed the nitrogen-boron DAP spectrum in 3C SiC and found that it is Type I, indicating that in the ***final state*** the ionized donor and acceptor charges occupy the same sublattice. Since nitrogen substitutes for carbon, a logical conclusion is that the deep boron level is associated with boron replacing carbon. This interpretation is called into question by recent data on B in 6H SiC obtained

[a]Electronic mail: devaty@pop.pitt.edu

using ESR and ENDOR,[11–15] which support a model for the deep boron center as a complex consisting of a boron atom replacing a silicon atom (B_{Si}) with an adjacent carbon vacancy (V_C). The $B_{Si}-V_C$ axis is along the *c* axis of the crystal. The optical and spin resonance data are consistent if the negative charge associated with the ionized acceptor in the final state of the DAP transition is centered on a carbon site. Kuwabara and Yamada[16] also measured the temperature dependence of the free conduction electron to neutral deep boron transition in 3C SiC. Based on the currently accepted value for the binding energy of the free exciton in 3C SiC, $E_X = 27$ meV,[17] the ionization energy for the deep boron center in 3C SiC is 748 meV. Ikeda *et al.*[18] interpreted features in photoluminescence spectra of 4H, 6H, and 15R SiC as nitrogen-boron distant DAP peaks, their phonon replicas, and free to bound boron transitions. For boron in 4H SiC, they estimated the ionization energy $E_A(\mathrm{B}) = E_X + 627$ meV. The binding energy of the free exciton is not known accurately for 4H SiC. Deep level transient spectroscopy (DLTS)[2,19] also reveals a deep boron-related level, associated with a complex named the *D* center. Analysis of double correlated DLTS[2,19] data indicates that the *D* center acts as a donor. It is not the purpose of this article to resolve the important questions as to whether the *D* center and the deep boron center observed by optical experiments are one and the same and, if so, whether this center is a donor or acceptor. Since the focus here is on results obtained by optical experiments, we shall regard the deep boron center as an acceptor.

Growth conditions determine the configurations and concentrations of boron related centers in SiC. For epitaxial growth by chemical vapor deposition (CVD), the site competition model[20,21] predicts that a low Si/C ratio favors the incorporation of B at silicon sites. Larkin *et al.*[21,22] have grown films by CVD which indeed show shallow silicon-site boron. In the present work, the Si/C ratio is adjusted to obtain films showing either shallow or deep boron centers in low temperature photoluminescence spectra.

Bound exciton spectra, particularly the sharp no-phonon lines, are important diagnostics for the characterization of SiC. This article reports the observation by low temperature photoluminescence (LTPL) of the recombination of a neutral acceptor (bound exciton) complex for silicon site boron observed in homoepitaxial films of 4H SiC grown by CVD. The no-phonon peak is at 3838 Å. We call this luminescence spectrum 4B. $4B_0$ refers to the no-phonon spectrum. A preliminary report[23] has been published. Section II discusses the growth of samples and the equipment used to characterize them. Section III discusses the shallow boron center. Selected samples are characterized using the temperature dependent Hall effect, admittance spectroscopy, and DLTS. The new LTPL spectrum is presented and arguments based on experiment are given in support of its identification as the 4B complex. Also discussed are some of the unusual properties of this spectrum, including its sensitivity to temperature. Section IV presents work on the DAP and FB luminescence associated with the deep boron acceptor and a determination of its ionization energy, offset by the unknown free exciton binding energy. Section V summarizes the conclusions.

II. EXPERIMENT

4H SiC epilayers were grown in a cold-wall, horizontal, atmospheric pressure CVD reactor.[24,25] The substrates were commercially available *n*-type 4H SiC boule-derived wafers, polished 3° off-axis from the (0001) Si-face basal plane.[26] The SiC substrates were precleaned using a standard degreasing solution, immersed in boiling sulfuric acid for ten minutes, rinsed in deionized water, and finally dried with filtered nitrogen. The cleaned substrates were placed onto a SiC-coated graphite susceptor and then loaded into a water-cooled fused silica reactor. The samples were heated via the radio frequency-coupled susceptor, which was temperature controlled at 1450 °C using an optical pyrometer. Silane (3% in H_2) and propane (3% in H_2) were used as the sources for SiC epilayer growth. The typical growth rate was 3 μm/h. Just prior to SiC CVD epitaxial growth, a 90 sccm flow of ultrapure hydrogen chloride gas in a 3 sLpm flow of hydrogen was used for a 1350 °C *in situ* etch for improved surface morphology.[27,28] All gases were mass flow controlled, including the ultrapure hydrogen carrier gas, which was purified using a heated-palladium diffusion cell.

Diborane (tank of 25 ppm B_2H_6 in H_2) was used as the source of boron for *p*-type doping. Capacitance–voltage ($C-V$) measurements were obtained at 1 MHz on a mercury-probe instrument with a mercury Schottky contact (contact area $= 1.64\times10^{-3}$ cm^2) using the mechanical sample-hold-down paddle as the electrical ground on the back of the sample. Site-competition epitaxy was utilized to ensure reproducibly doped CVD SiC epitaxial layers.[20] This previously reported technique for controlled dopant incorporation is based on adjusting the silicon-source/carbon-source flow ratio (Si/C ratio) within the crystal growth reactor during epitaxial growth to affect dopant incorporation into a growing SiC epitaxial layer. For example, on both 4H and 6H SiC (0001) Si-face substrates, the concentration of nitrogen dopant incorporated is proportional to the Si/C ratio whereas phosphorus, boron, and aluminum dopant incorporation is inversely proportional to the Si/C ratio used in the CVD reactor during epitaxial growth.[22,29]

We used the temperature dependence of the Hall effect[30] and admittance spectroscopy[31] to verify that samples showing the 3838 Å photoluminescence peak are indeed doped with shallow boron. In addition, the Hall effect, admittance spectroscopy, and DLTS[32] were used to determine electrical parameters including the boron concentration, boron ionization energy, concentration of the compensation, Hall mobility, and resistivity. For the Hall effect measurements, we prepared Ohmic contacts in a van der Pauw arrangement by evaporating Al and subsequently annealing for five minutes at $T = 950$ °C. To avoid leakage currents around the *p-n* junction (*p*-type CVD epilayer on *n*-type substrate), we fabricated mesa structures by removing an edge zone on the sample surface of approximately 5 μm in depth by reactive ion etching. Ni Schottky contacts, diameter 0.57 mm, were deposited by vacuum evaporation for the admittance spec-

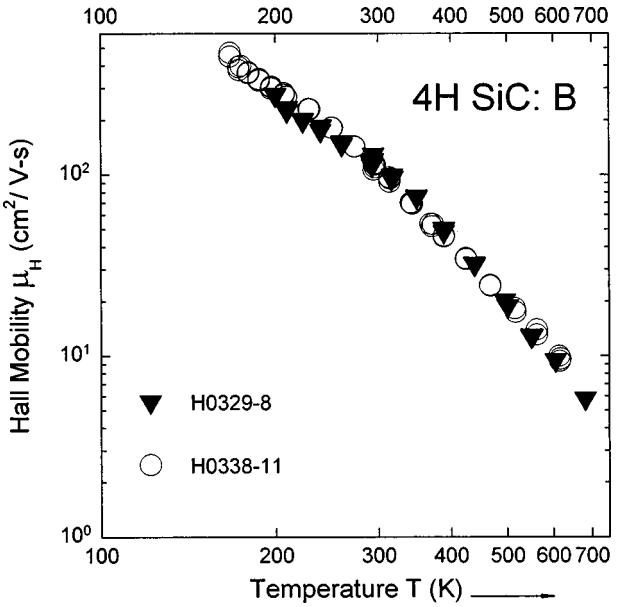

FIG. 1. Temperature dependence of the Hall hole mobility for two homoepitaxial 4H SiC films doped with boron during CVD growth.

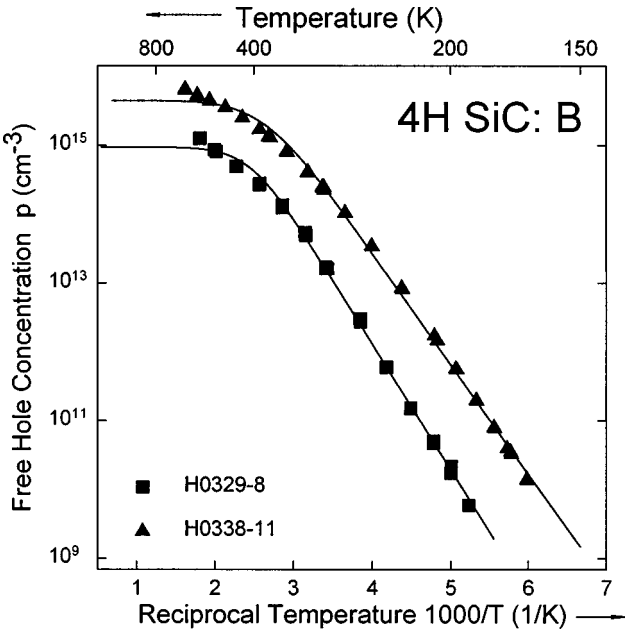

FIG. 2. Temperature dependence of the free hole concentration for two homoepitaxial 4H SiC films doped with boron during CVD growth. The symbols indicate the data measured using the Hall effect. The lines indicate the least square fits of the neutrality equation to the data.

troscopy and DLTS measurements. The Al Ohmic contacts were used as ''backside'' contacts. We performed the Hall effect and DLTS measurements over the temperature range 150–700 K, and admittance spectroscopy over 30–350 K.

Photoluminescence spectra were recorded using primarily a charge coupled device array detector on either a 3/4 meter Fast-Fastie or a 2 m Baird-Atomic spectrometer. Most spectra were measured with the sample immersed in a liquid helium bath pumped down to 2 K, or at room temperature. Intermediate temperatures, indicated on the figures, were obtained using a Janis Super VariTemp cryostat. Spectra showing the temperature dependence of the conduction electron to neutral boron FB peak were measured on a 3/4 meter SPEX monochromator using a thermoelectrically cooled RCA C31034 A photomultiplier tube and photon counting. The excitation sources for luminescence were a 46 mW He–Cd laser (3250 Å) or a 60–70 mW frequency doubled argon ion laser (2440 Å). The attenuation lengths[33] of the laser radiation (reciprocals of the absorption coefficients) for the two sources are 8.6 and about 0.15 μm, respectively, in 4H SiC.

III. SHALLOW BORON CENTER

Figures 1 and 2 show the temperature dependence of the Hall mobility μ_H and the free hole concentration p, respectively, for two samples which show sharp $4B_0$ no-phonon lines. The Hall mobility is determined from the measured Hall constant R_H and resistivity ρ using

$$\mu_H = \frac{|R_H|}{\rho}. \tag{1}$$

The free hole concentration is

$$p = \frac{r_{H,p}}{eR_H}, \tag{2}$$

where $r_{H,p}$ is the Hall scattering factor for holes, assumed equal to one independent of temperature, and e the electron charge. These samples show high hole mobility and low resistivity. The neutrality equation for a nondegenerate p-type semiconductor with a single acceptor level is

$$p + N_{\text{comp}} = \frac{N_A}{1 + \frac{gp}{N_V}\exp(\Delta E/kT)}, \tag{3}$$

where N_A is the concentration of acceptors, ΔE their ionization energy, g the degeneracy of the acceptor ground state, N_V the effective valence band density of states, N_{comp} the concentration of compensating states, T the absolute temperature, and k Boltzmann's constant. By setting $g=4$ we assume that there are four (including spin) degenerate impurity levels which contribute in the neutrality equation. We use the temperature dependent density of states effective mass for the valence bands of 4H SiC computed by Wellenhofer and Rössler[34] to calculate N_V. The most significant consequence of replacing the free electron mass with the density of states effective mass is an increase of about a factor of 10 in the compensation. Figure 2 shows the best fits of the neutrality equation to the data. Table I displays the measured and derived parameters for the two samples. Based on the ionization energies determined by the fit, the p-type conductivity of both CVD layers is determined by the shallow boron acceptor. The compensation is significant. Simulations reveal that it is not possible to detect the deep boron acceptor using temperature dependent Hall measurements over the accessible temperature range of our equipment.

Admittance measurements were performed in the frequency range 10 kHz–2 MHz to verify the presence of shallow boron and to check the value of the ionization energy.

TABLE I. Results from Hall Effect measurements on boron-doped 4H SiC films.

Sample	H0338-11	H0329-8
ρ(295 K) (Ω cm)	225	3222
$\rho_{\min}$ (Ω cm)	72 (469 K)	359 (606 K)
μ_H (295 K) (cm^2/V s)	114	116
$\mu_{H,\max}$ (cm^2/V s)	470 (167 K)	277 (200 K)
$N_A(B)$ (cm^{-3})	$(8.9\pm1.8)\times10^{15}$	$(3.9\pm0.8)\times10^{15}$
N_{comp} (cm^{-3})	$(4.4\pm0.9)\times10^{15}$	$(2.9\pm0.6)\times10^{15}$
$\Delta E(B)$ (meV)	291 ± 10	332 ± 10

Figure 3 shows a peak in the normalized conductance, previously observed[2] in 4H SiC films doped with boron during CVD growth. These curves are analyzed to obtain a temperature dependent time constant $\tau(T)$. A value for the ionization energy of the shallow boron center ΔE is obtained using the expression

$$\tau = \frac{1}{2N_V\sigma_p v_{\text{th},p}} \exp\left[\frac{\Delta E}{kT}\right], \tag{4}$$

where σ_p is the capture cross section and $v_{\text{th},p}$ the thermal velocity for holes. We assume that $N_V \sim T^{3/2}$ and $v_{\text{th},p} \sim T^{1/2}$. A power law dependence is assumed for the capture cross section for holes: $\sigma_p \sim T^{\alpha}$ with $\alpha = -2$ for cascade capture[35] and $\alpha = 0$ for multiphonon capture.[36] Figure 4 shows the best fits obtained assuming cascade capture. Table II lists the ionization energies. The values obtained assuming cascade capture differ only slightly from those obtained by the Hall effect. Ionization energies of shallow impurities (Al, N, and P) determined using admittance and the Hall effect agree well assuming cascade capture, but the agreement is poorer assuming multiphonon capture.

Figure 5 shows DLTS data on sample H0338-11. The peak near 300 K is attributed to the deep boron related center

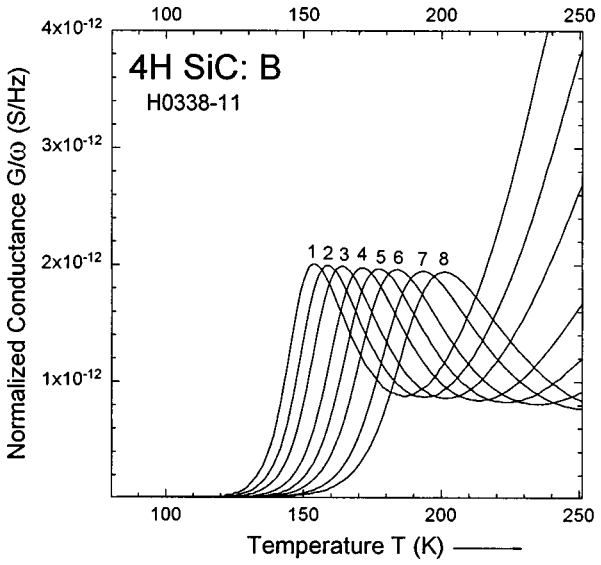

FIG. 3. Temperature dependence of the normalized conductance of a homoepitaxial 4H SiC film doped with boron during CVD growth, measured by admittance spectroscopy. The curves were measured at the frequencies: (1) 10 kHz; (2) 20 kHz; (3) 40 kHz; (4) 100 kHz; (5) 200 kHz; (6) 400 kHz; (7) 1 MHz; 8: (2) MHz.

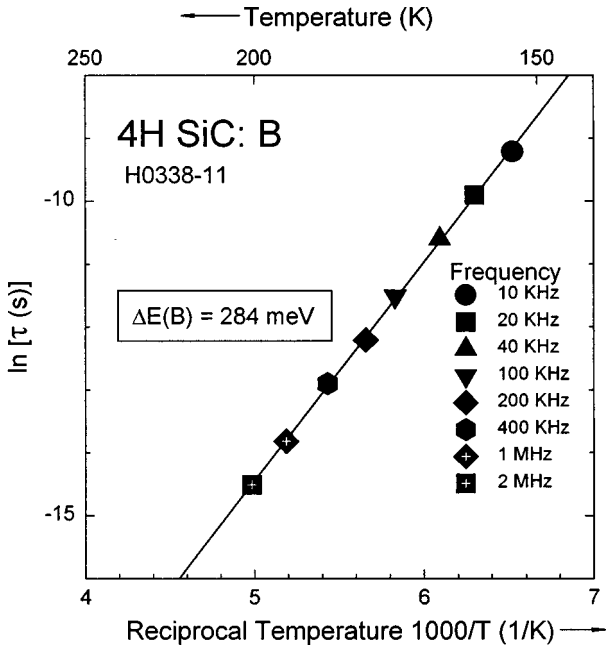

FIG. 4. Logarithm of the time constant, obtained by analysis of the admittance spectroscopy data shown in Fig. 3, plotted against reciprocal temperature. The symbols indicate the frequencies at which admittance spectroscopy was performed. The slope of the line passing through the data points provides the value 284 meV for the ionization energy of the shallow boron center in 4H SiC.

(D center).[19] The energy position is 498 ± 9 meV (550 ± 9 meV) above the top of the valence band, assuming $\sigma_{n,p} \propto T^0$ ($\sigma_{n,p} \propto T^{-2}$). The concentration of the deep boron center in this sample evaluated from the DLTS peak height is $(1.3\pm0.2)\times10^{13}$ cm^{-3}, which is low. No other deep center is detected in the lower half of the band gap. This DLTS measurement is not sensitive to the shallow boron center. The concentration of the D center in sample H0329-8 is $(2-4)\times10^{14}$ cm^{-3}, estimated using DLTS data.

We now discuss the photoluminescence data. A peak near 3838 Å is observed in the LTPL spectrum of boron doped 4H SiC epitaxial films grown using a low Si/C ratio. For some samples, this peak is quite sharp. Figure 6 shows LTPL spectra of boron doped 4H SiC films grown using low and high Si/C ratios with a relatively low nitrogen background doping. The sharp peaks labeled P_0 and Q_0 are the no-phonon lines of the neutral nitrogen donor four particle (bound exciton) complex[37] 4N for nitrogen substituting on the inequivalent hexagonal and quasicubic carbon sites. The reduced strength of the nitrogen lines for the film grown with low Si/C ratio is consistent with site-competition epitaxy,

TABLE II. Ionization energies of the shallow boron acceptor in 4H SiC from admittance spectroscopy (uncertainty: ±10 meV).

Sample	H0338-11	H0329-8
$\Delta E(B)$ (meV)	259	262
Multiphonon capture: $\sigma_p \propto T^0$		
$\Delta E(B)$ (meV)	284	295
Cascade capture: $\sigma_p \propto T^{-2}$		

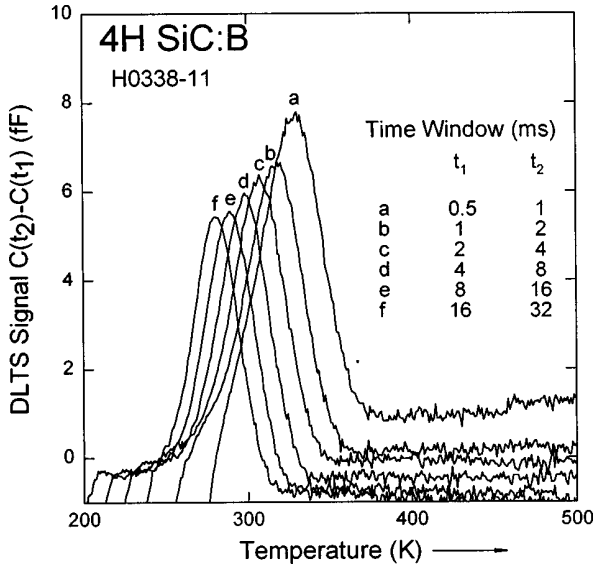

FIG. 5. DLTS signal for an homoepitaxial 4H SiC film doped with boron during CVD growth. The time windows, in ms, used to obtain the curves are indicated on the plot.

since growth under these conditions favors the incorporation of impurities at the Si sites. The peak at 3838 Å, labeled $4B_0$, is due to the no-phonon recombination of a four particle complex associated with the shallow boron center. The appearance of this peak for low Si/C growth conditions suggests an association with the Si site according to site-competition epitaxy.

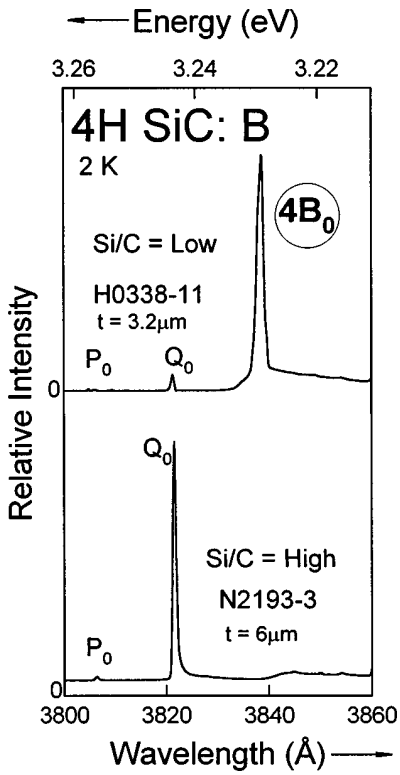

FIG. 6. Low temperature photoluminescence spectra of two boron-doped 4H SiC epitaxial films, thicknesses t, grown using two different Si/C source gas ratios. The peaks labeled P_0 and Q_0 are no-phonon lines of the neutral nitrogen donor four particle complex at the hexagonal and quasicubic sites, respectively. The sharp peak labeled $4B_0$ is due to no-phonon recombination of the neutral shallow boron four particle bound exciton complex. The zero level for each spectrum is indicated at the left of the figure. The changes in the spectra are consistent with site-competition epitaxy for nitrogen substituting for carbon and boron for silicon.

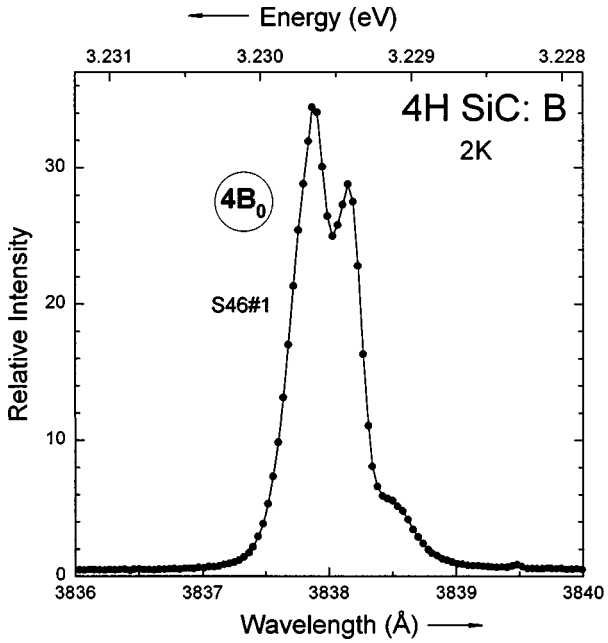

FIG. 7. High resolution spectrum of $4B_0$ showing at least three closely spaced lines.

There are at least two no-phonon lines in the LTPL spectra for Al[38,39] and Ga[40,41] neutral acceptor four particle complexes in 4H SiC. When measured at high resolution (Fig. 7), the sharp $4B_0$ peak splits into at least three lines for some samples. Since this splitting is not yet understood, we postpone discussion to a future publication.

To establish a correlation between the intensity of the 3838 Å peak and boron doping, two epitaxial layers were grown separately using the same Si/C ratio. The diborane flow differed by a factor of 2. The intensity of the feature labeled $4B_0$ grows with added boron, as shown in Fig. 8. Although the nitrogen $4N_0$ and aluminum (labeled $4Al_0$) no-phonon lines are sharp, the $4B_0$ feature is quite broad, which is typical of most of the samples we have examined, but not yet explained. The large variation in the width of $4B_0$ suggests that this complex is very sensitive to environmental conditions such as local strains and to growth conditions. The structure riding on the long wavelength tail of $4B_0$, which does not grow with added diborane, is due to momentum conserving phonon replicas of P_0.

Figure 9 shows LTPL spectra for two 4H SiC films grown with different Si/C ratios. The meanings of values of Si/C are reactor-specific. They are given here only to indicate the qualitative trend. The Si/C ratio was adjusted by changing only the carbon source flow rate while maintaining constant flow rates for the boron and silicon sources. The relative strengths of P_0 and Q_0 with respect to $4B_0$ are consistent with site-competition epitaxy if $4B_0$ is associated with Si sites.

Momentum conserving (MC) phonon replicas of neutral acceptor bound exciton recombination are observed in LTPL spectra for samples which contain unusually low concentra-

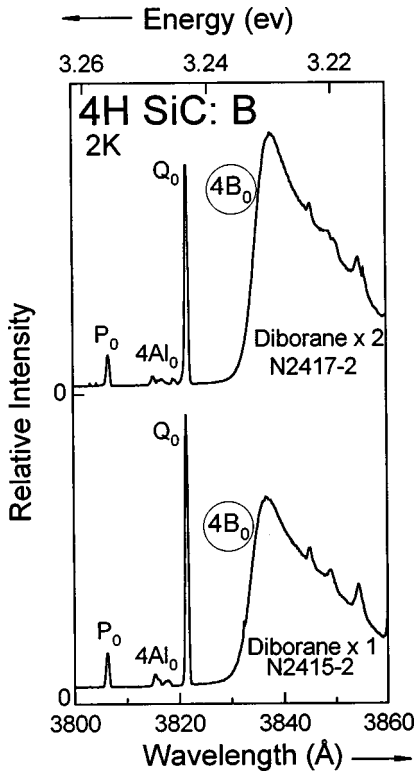

FIG. 8. Low temperature photoluminescence spectra of two boron-doped 4H SiC epitaxial films, grown using the same low Si/C source gas ratio. Twice as much diborane was added to the flow during CVD growth of the sample whose spectrum is shown at the top of the figure. The peaks labeled P_0 and Q_0 are no-phonon lines of the neutral nitrogen donor four particle complex. Note $4Al_0$ labels the no-phonon spectrum of the neutral aluminum acceptor four particle complex. The broad peak labeled $4B_0$ is due to the recombination of a neutral shallow boron acceptor four particle complex. The zero level for each spectrum is shown at the left of the figure. The spectral features riding on the long wavelength tail of $4B_0$, which do not change with added boron, are phonon replicas of P_0.

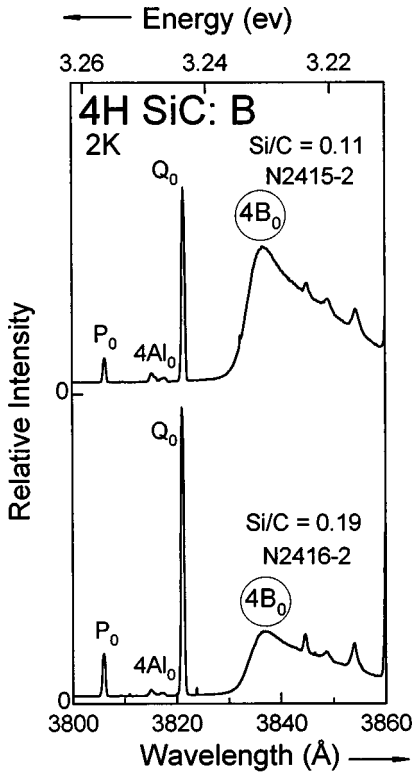

FIG. 9. Low temperature photoluminescence spectra of two boron-doped 4H SiC epitaxial films, grown using two different Si/C source gas ratios. The values of the ratios are reactor specific and provided only to indicate the trend. See the caption of Fig. 8 for notation of labels. The zero level for each spectrum is shown at the left of the figure. The features riding on the long wavelength tail of $4B_0$ are phonon replicas of P_0. The differences between the two spectra are consistent with site-competition epitaxy for carbon site nitrogen and silicon site boron.

tions of nitrogen (Fig. 10). The boron-doped boule sample shows strong MC phonon replicas of $4B_0$. The weak no-phonon spectrum of the neutral aluminum acceptor four particle complex ($4Al_0$) is also present. The epitaxial film contains both B and Al, and the lines of the shallower Al centers dominate the MC phonon replicas. Although the observed 4B MC phonon replica lines are broad, the energies of the MC phonons are consistent with those of the 4Al spectrum.

Figure 11 shows the no-phonon spectrum of the shallow boron center for sample H0338-11, which exhibits a sharp $4B_0$ peak at $T=2$ K, measured at five temperatures ranging from 7 to 47 K. An excited state transition (or band), shifted 2.8 ± 0.2 meV higher in energy, appears and is in fact the dominant feature for $T\geqslant13$ K. Although there are only three temperatures, the intensities of these peaks are related by the Boltzmann factor $e^{-\Delta E/kT}$ with $\Delta E=2.2$ meV. There is also a high energy shoulder, most prominent on the 23 K spectrum, which may indicate an additional excited state or band. The intensity of the spectrum drops dramatically between 23 and 37 K. For comparison, Fig. 12 shows the temperature dependence of the $4Al_0$ spectrum in 4H SiC. In contrast with $4B_0$, at $T=2$ K (not shown) this spectrum is a doublet, possibly associated with no-phonon recombination at the two

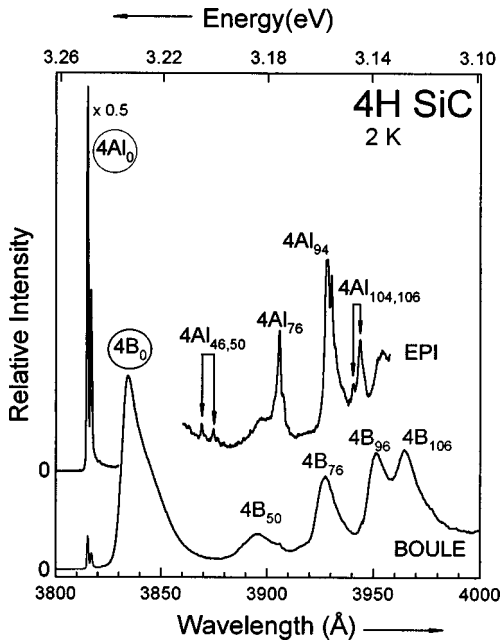

FIG. 10. LTPL spectra of an unintentionally doped 4H SiC epitaxial film (top) and a 4H SiC boule sample (bottom), both with very low nitrogen background. Peaks labeled 4Al and 4B are no-phonon and phonon replica transitions due to recombination of the neutral aluminum and neutral shallow boron acceptor four particle bound exciton complexes, respectively. The energies of momentum conserving phonons are indicated in meV. The zero level for each spectrum is shown at the left of the figure. The 4B replicas are prominent in the lower spectrum because the aluminum concentration is low in the boule sample.

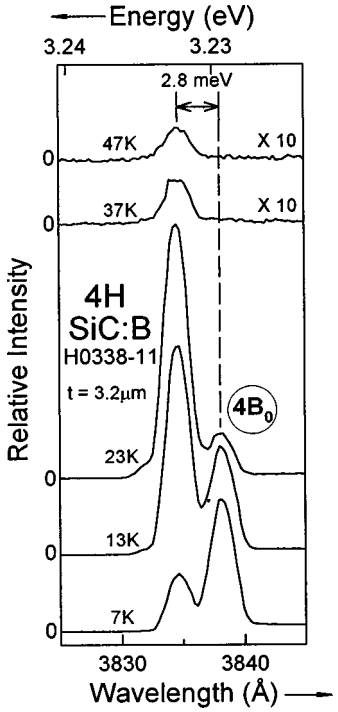

FIG. 11. Temperature dependence of the $4B_0$ photoluminescence spectrum. The zero for each spectrum is shown at the left. As the temperature is raised, excited state transitions grow in strength. The integrated intensity drops precipitously between 23 K and 37 K. The film thickness is 3.2 μm.

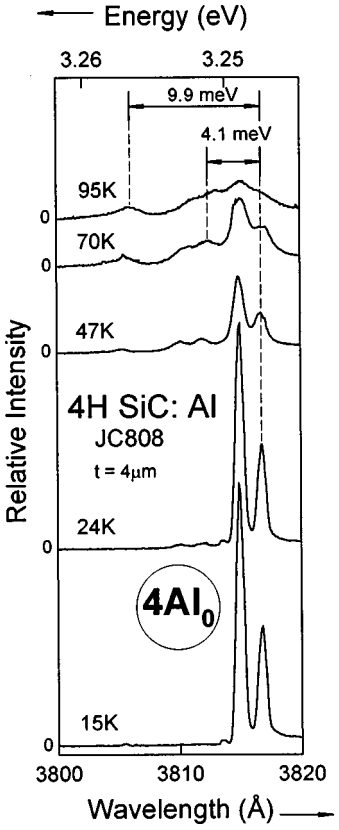

FIG. 12. Temperature dependence of the $4Al_0$ photoluminescence spectrum. The zero for each spectrum is shown at the left. Excited state transitions grow in strength with increasing temperature. Although there is considerable broadening of the lines, the integrated intensity does not decrease much between 15 and 95 K. The film thickness is 4 μm.

inequivalent Si sites. As the temperature increases, an excited state doublet appears, shifted by 4.1 ± 0.2 meV from the doublet observed at 2 K. For the spectra taken at $T \geqslant 47$ K, there is an additional peak shifted 9.9 meV from the lowest energy peak. There is also a small peak just above the low temperature doublet on the 15 and 24 K spectra. This peak is not observed in the spectra measured at higher temperatures, possibly due to broadening.

A comparison of Figs. 11 and 12 reveals significant differences in behavior between the $4B_0$ and $4Al_0$ spectra with increasing temperature. First, the intensity of the 2.8 meV excited state exceeds that of the 3838Å line in $4B_0$ for $T \geqslant 13$ K, whereas the $4Al_0$ lines observed at 2 K remain the most intense at 95 K, although they are thermally broadened. Second, although the exciton binding energy to the acceptor is greater for 4B (35 meV) than 4Al, its intensity is quenched by almost two orders of magnitude by 37 K. In contrast, the integrated area under the $4Al_0$ spectrum has hardly decreased at all at this temperature, as shown in Fig. 13. The points for $4Al_0$ include data for two different samples.

Because the covalent radius of B (0.82 Å) is considerably smaller than for Si (1.11 Å), there is the possibility of relaxation of the B atom to an off-center location as well as distortion of the positions and bonding of the nearby atoms. ESR and ENDOR data on B replacing Si in 3C,[3,5,6] 6H,[3,4,7,8] and 4H SiC[3,9] are interpreted using models[6–8,42,43] based on this idea. According to the model which has gained the most recent favor,[7,43] at low temperatures one of the boron-carbon bonds is stretched. The boron atom relaxes towards a planar configuration and is bonded with its three nearest neighbor carbon atoms. The carbon atom also relaxes and is bonded with its three nearest silicon neighbors. The unpaired spin in the neutral complex is partly localized on the dangling carbon p-orbital directed towards the boron, and partly delocalized in the surrounding lattice. The boron itself is neutral in

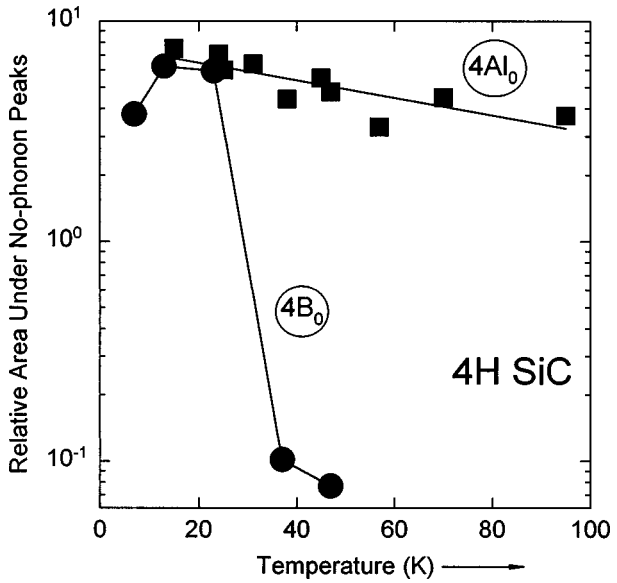

FIG. 13. Temperature dependence of the relative area under the no-phonon peaks for the $4B_0$ and $4Al_0$ spectra. Note the quenching of the $4B_0$ spectrum, measured for Sample H0338-11, between 20 and 37 K.

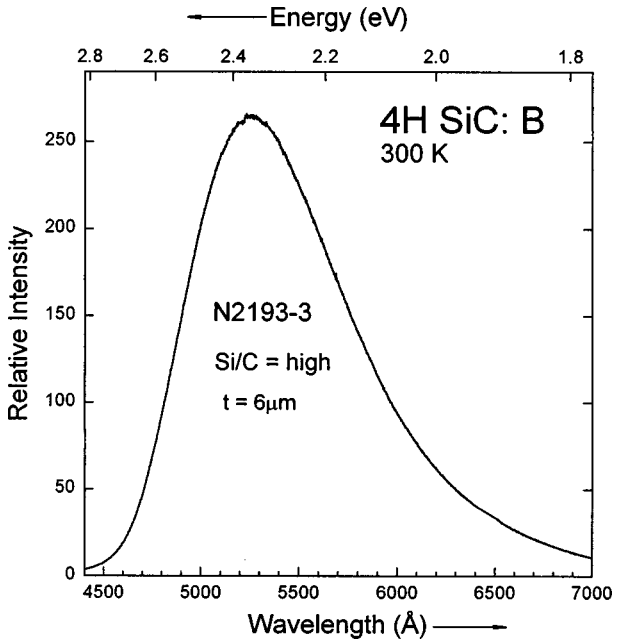

FIG. 14. Room temperature photoluminescence spectrum of a boron-doped 4H SiC homoepitaxial film, 6 μm thick, grown using a high Si/C ratio. The broad band peaked in the green is boron related.

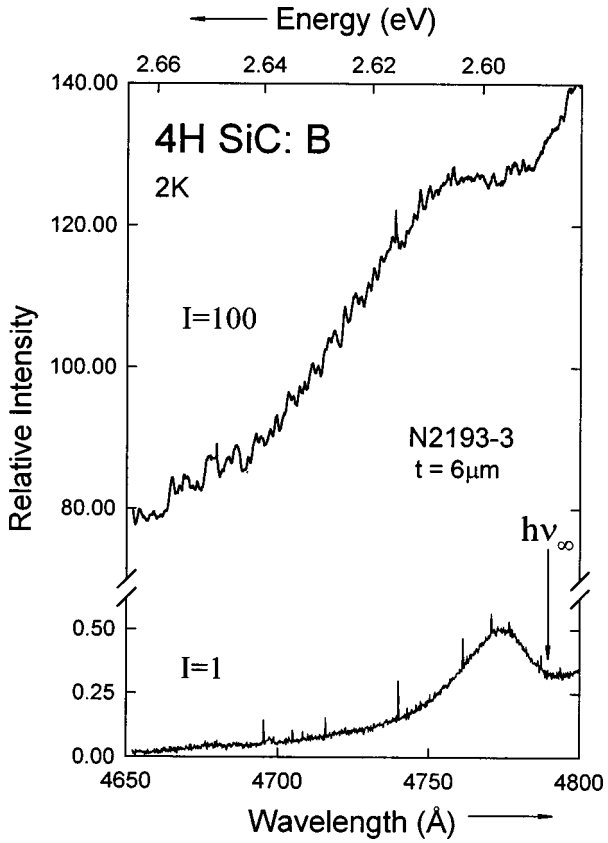

FIG. 15. LTPL spectra of the boron-doped 4H SiC film (Sample N2193-3), 6 μm thick, measured using two different intensities of 325 nm HeCd laser excitation. The top spectrum, obtained using a relatively high excitation intensity, shows detailed donor-acceptor pair shell structure as well as the distant pairs peak. The lower spectrum, measured using an excitation intensity reduced by a factor of 100, does not show the shell structure. Also, the peak is shifted to a longer wavelength due to reduced saturation of distant pairs. $h\nu_\infty$ is the estimated energy of the emitted photon in the limit of infinite separation between the donor and acceptor.

this model. The ESR data on boron in 6H SiC[7] and 4H SiC[9] suggest that at low temperatures the relaxation takes place along an axial bond for the hexagonal site, but along a non-axial bond for the quasicubic sites. Thus, for 4H SiC, the carbon atom carrying much of the unpaired spin is on the hexagonal site (before relaxation) for boron replacing silicon at both the hexagonal and quasicubic sites. As the temperature increases, there may be a transition from a specific distorted configuration to a dynamic state involving reorientation among several configurations. The dynamic reorientation may not permit the binding of an exciton to the complex, leading to the observed thermal quenching of the luminescence. Zubatov *et al.*[3] and Greulich-Weber *et al.*[9] performed ESR studies of the shallow boron center in 4H–SiC. Zubatov *et al.*[3] refer to the two centers associated with boron replacing silicon at the quasicubic and hexagonal sites as B_2 and B_3, respectively. Their values of the g-tensor of the B_2 spectrum change between 35 and 50 K,[3] which corresponds reasonably with the thermal quenching of the $4B_0$ luminescence spectrum.

The origin of the excited states of $4B_0$ is not understood. Because they are thermally excited, the excited states are associated with the four particle complex (initial states) rather than the neutral acceptor (final states). There are a number of possibilities, including excitation of the electron into a higher valley orbit state, or some other electronic state such as a $2p$-like state, or excitation of one of the holes into the next valence band, split off by the spin orbit interaction (assuming that the hole can be described by effective mass theory).

IV. DEEP BORON CENTER

4H SiC films doped with boron during CVD growth with a low Si/C ratio show the shallow boron 4B spectrum, whereas films grown under Si-rich conditions show boron-related donor-acceptor pair and free-to-bound spectra associated with a deep acceptor (ionization energy $\sim$650 meV).

Figure 14 shows the room temperature photoluminescence spectrum measured over a broad range of wavelengths for a boron-doped 4H SiC film (Sample N2193-3) grown by CVD using a high Si/C ratio. The broad photoluminescence spectrum peaked in the green[44] is similar to the electroluminescence spectrum for boron-doped 4H SiC light-emitting diodes.[45] The broad peak is not observed for films grown at low Si/C ratios.

The photoluminescence spectrum at $T=2$ K for the same sample of boron-doped 4H SiC in the region near the short wavelength edge of the broad peak shows many sharp peaks, which are not noise but part of the nitrogen-deep boron DAP spectrum (Fig. 15). Yamada and Kuwabara[10] analyzed the N–B DAP spectrum of 3C SiC and concluded that the participating boron acceptors replace carbon. As discussed in Section I, recent electron spin resonance and ENDOR data[11–15] are interpreted using a different model. Unfortunately, the shell structure of DAP's is more complex in 4H SiC than for 3C SiC, so that it has not been possible to analyze the N–B DAP spectrum in detail. Each sublattice in

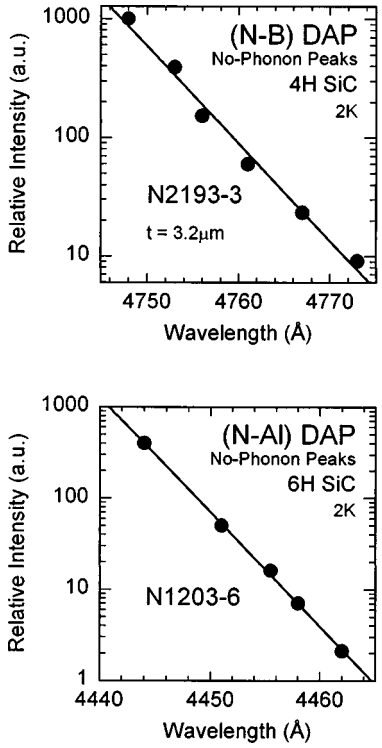

FIG. 16. Intensity of 325 nm HeCd laser excitation plotted against the wavelength of the no-phonon distant pairs peak measured at $T=2$ K for 4H SiC nitrogen-boron (Sample N2193-3, film thickness 3.2 μm, top panel) and 6H SiC nitrogen-aluminum (bottom panel) donor-acceptor pair transitions.

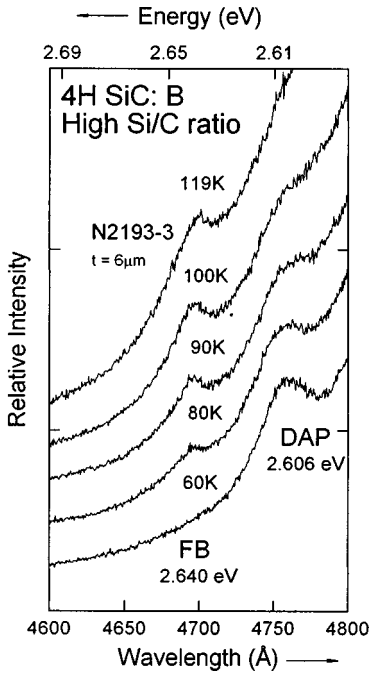

FIG. 17. Temperature dependence of the photoluminescence spectrum of a boron-doped 4H SiC film (Sample N2193-3), 6 μm thick, grown by CVD using a high Si/C ratio. The no-phonon peaks of the DAP, and conduction electron to neutral deep boron acceptor FB transitions are labeled. As the temperature increases, nitrogen donors are thermally ionized, leading to the disappearance of the DAP peak and the growth of the FB peak.

4H SiC has two inequivalent sites, one hexagonal (h) and the other quasicubic (k). The ionization energy for nitrogen substituting for carbon in SiC is strongly site dependent. However, the site dependence of deep boron acceptor ionization energies is not known. It is likely that the observed DAP spectrum is actually four superposed spectra, corresponding to the combinations D_h-A_h, D_h-A_k, D_k-A_h, and D_k-A_k, where D and A denote donor and acceptor, respectively, and subscripts identify the sites.

Figure 15 shows the 4H SiC nitrogen-boron no-phonon DAP LTPL spectrum for Sample N2193-3, including the distant pairs peak. Note that sharp lines ride on top of the distant pairs peak for the top curve, measured using a higher excitation intensity. These lines may arise from pairs for which the nitrogen is on the k site, where it has a larger ionization energy.[46] The distant pairs peak shifts to longer wavelengths as the intensity of the excitation is reduced, as shown in Fig. 15. For the spectrum taken with the intensity reduced by a factor of 100, the sharp line spectrum is not observed and the emission intensity is reduced by more than a factor of 100. The radiative recombination rate of a DAP depends strongly on the distance separating the donor and acceptor, especially for distant pairs for which only the exponentially decaying tails of the wave functions of the bound electron and hole overlap. Due to the slow recombination rates, the lines due to distant pairs saturate with increasing intensity, leading to a shift of the peak towards closer pairs, which recombine more quickly.

The measured dependence of the wavelength λ of the no-phonon nitrogen-boron distant pairs peak in 4H SiC on excitation intensity I is shown in Fig. 16. A linear dependence is observed when the data are plotted using semilogarithmic axes, suggesting a dependence $\lambda=\lambda_0 \ln(I/I_0)$ where λ_0 and I_0 are constants. Figure 16 also shows that a similar dependence is observed for N–Al pairs in 6H SiC. The intensity dependence of the wavelength position of the distant DAP peak has been studied in other semiconductors[47–51] and models have been proposed.[50,52]

The intensity of the no-phonon DAP peak decreases with increasing temperature as the shallow nitrogen donors are ionized (Fig. 17). A new peak appears for temperatures above 60 K, which we assign to conduction electron to neutral deep boron FB transitions. Samples which show strong DAP luminescence also show strong FB transitions.

The FB luminescence may be analyzed to provide an estimate of the ionization energy of the deep boron acceptor. Figure 18 shows the temperature dependence of the FB peak energy E_{PEAK}, after correction for the temperature dependence of the exciton band gap E_{GX}.[53] A simple model[54] predicts the temperature dependence

$$E_{\mathrm{PEAK}}(T)=E_G(T)-E_A+ckT, \tag{5}$$

where E_G is the band gap and E_A the acceptor binding energy. The coefficient $c=a+1$, where a is the exponent for the assumed power law dependence of the electron capture cross section on energy: $\sigma(E)\propto E^a$, with E measured from the bottom of the conduction band. The data plotted in Fig. 18 are consistent with $c=0.5$, which is also the value for the aluminum acceptor in 4H SiC.[18,39] The physical origin of the value $c=1/2$ is discussed in the literature.[55–57] When extrapolated to zero temperature, the data indicate E_{GX}

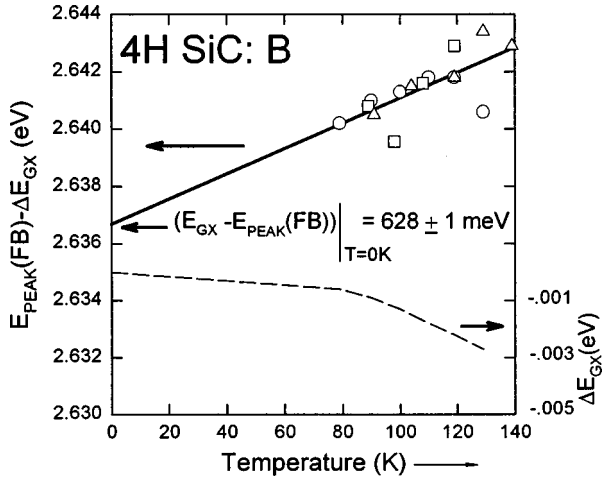

FIG. 18. Analysis of nitrogen-deep boron FB transitions for boron-doped 4H SiC epitaxial films. The symbols show the energy of the FB peak, corrected for the temperature dependence of the exciton gap, as a function of temperature. Each type of symbol indicates a specific sample. The dotted line shows the decrease of the exciton band gap with increasing temperature. The solid line is a fit to the data. Extrapolation of this line to zero temperature leads to the value 628 ± 1 meV. The exciton binding energy, not reliably known for 4H SiC, must be added to this value to obtain the ionization energy of the deep boron acceptor.

$-E_{\mathrm{PEAK}}=E_A-E_X=628\pm1$ meV, where $E_{\mathrm{GX}}+E_X=E_G$. The binding energy of the free exciton E_X is required to obtain E_A. A reliable value of E_X is not yet available for 4H SiC. The value $E_X=27$ meV for 3C SiC[17] may be used to estimate $E_A(B)=655$ meV for the deep boron center in 4H SiC.

The nitrogen-deep boron DAP spectrum measured at low excitation intensity (Fig. 15) may be analyzed to provide a corroborating, but less accurate, estimate for the binding energy of the deep boron acceptor. The energy of the emitted photon in the limit of infinite separation between the donor and acceptor, $h\nu_\infty$, is related to the donor and acceptor ionization energies by[58]

$$h\nu_\infty=E_g-(E_D+E_A). \tag{6}$$

The binding energy obtained by infrared absorption[46] for the nitrogen donor substituting at the hexagonal carbon site, the shallower of the two nitrogen donor levels in 4H SiC, is about 52 meV. The exciton bandgap[37] for 4H SiC at 2 K is $E_{GX}=E_G-E_X=3.265$ eV. Using $h\nu_\infty=2.588$ eV, corresponding to the minimum beyond the peak (Fig. 15, $I=1$ spectrum), $E_A=625$ eV$+E_X$.

V. CONCLUSION

We have presented and discussed photoluminescence spectra related to both a shallow boron acceptor associated with silicon sites and a deep boron acceptor in 4H SiC. The identification of the recombination of the neutral shallow boron acceptor four particle complex in the low temperature photoluminescence spectrum of 4H SiC provides a useful optical signature for identifying shallow boron in boule and CVD grown material. Additional work is required to understand the configurational and electronic structure of this center as well as its temperature dependence. Application of perturbation spectroscopies such as the work on magneto-optical photoluminescence now in progress in our laboratory and the extension of this investigation to include all the important SiC polytypes should provide important clues.

Regarding the deep boron center, no spectrum due to the recombination of a deep neutral acceptor four particle complex has yet been observed. However, the donor-acceptor pair and conduction electron to neutral acceptor free-to-bound transitions provide important information about the deep boron center. Further experimental work on the deep boron center using nonoptical techniques such as ESR and ENDOR is also necessary.

ACKNOWLEDGMENTS

The authors would like to thank J. Schmidt and A. Duijn-Arnold for informative discussions concerning the relationships between spin resonance data and photoluminescence spectra. This work was supported by the Office of Naval Research (Colin E. C. Wood, monitor) and the National Aeronautics and Space Administration.

[1] G. A. Lomakina, Sov. Phys. Solid State **7**, 475 (1965) [Fiz. Tverd. Tela (Leningrad) **7**, 600 (1965)].
[2] T. Troffer, Ch. Häßler, G. Pensl, K. Hölzlein, H. Mitlehner, and J. Völkl, Inst. Phys. Conf. Ser. **142**, 281 (1996).
[3] A. G. Zubatov, I. M. Zaritskii, S. N. Lukin, E. N. Mokhov, and V. G. Stepanov, Sov. Phys. Solid State **27**, 197 (1985) [Fiz. Tverd. Tela (Leningrad) **27**, 322 (1985)].
[4] T. L. Petrenko, V. V. Teslenko, and E. N. Mokhov, Sov. Phys. Semicond. **26**, 874 (1992) [Phys. Tekh. Poluprovodn. **26**, 1556 (1992)].
[5] V. Bratus', N. Baran, V. Maksimemko, T. Petrenko, and V. Romanenko, Mater. Sci. Forum **143–147**, 81 (1994).
[6] N. P. Baran, V. Ya. Bratus', A. A. Bugai, V. S. Vikhnin, A. A. Klimov, V. M. Maksimenko, T. L. Petrenko, and V. V. Romanenko, Phys. Solid State **35**, 1544 (1993).
[7] T. Matsumoto, O. G. Poluektov, J. Schmidt, E. N. Mokhov, and P. G. Baranov, Phys. Rev. B **55**, 2219 (1997).
[8] R. Müller, M. Feege, S. Greulich-Weber, and J.-M. Spaeth, Solid State Commun. **8**, 1377 (1993).
[9] S. Greulich-Weber, F. Feege, K. N. Kalabukhova, S. N. Lukin, J.-M. Spaeth, and F. J. Adrian, Semicond. Sci. Technol. **13**, 59 (1998).
[10] S. Yamada and H. Kuwabara, in *Silicon Carbide 1973* (University of South Carolina Press, Columbia, SC, 1974), p. 305.
[11] P. G. Baranov and E. N. Mokhov, Semicond. Sci. Technol. **11**, 489 (1996).
[12] P. G. Baranov and E. N. Mokhov, Phys. Solid State **38**, 798 (1996).
[13] P. G. Baranov, I. V. Ilyin, and E. N. Mokhov, Solid State Commun. **100**, 371 (1996).
[14] P. G. Baranov, E. N. Mokhov, A. Hofstetter, and A. Sharmann, JETP Lett. **63**, 848 (1996) [Pis'ma Zh. Eksp. Teor. Fiz. **63**, 803 (1996)].
[15] A. Duijn-Arnold, T. Ikoma, O. G. Poluektov, P. G. Baranov, E. N. Mokhov, and J. Schmidt, Phys. Rev. B **57**, 1607 (1998).
[16] H. Kuwabara and S. Yamada, Phys. Status Solidi A **30**, 739 (1975).
[17] D. Bimberg, M. Altarelli, and N. O. Lipari, Solid State Commun. **40**, 437 (1981).
[18] M. Ikeda, H. Matsunami, and T. Tanaka, Phys. Rev. B **22**, 2842 (1980).
[19] W. Suttrop, G. Pensl, and P. Lanig, Appl. Phys. A: Solids Surf. **51**, 231 (1990).
[20] D. J. Larkin, P. G. Neudeck, J. A. Powell, and L. G. Matus, Appl. Phys. Lett. **65**, 1659 (1994).
[21] D. J. Larkin, Inst. Phys. Conf. Ser. **142**, 23 (1996).
[22] D. J. Larkin, S. G. Sridhara, R. P. Devaty, and W. J. Choyke, J. Electron. Mater. **24**, 289 (1995).
[23] S. G. Sridhara, D. G. Nizhner, R. P. Devaty, W. J. Choyke, T. Troffer, G. Pensl, D. J. Larkin, and H. S. Kong, Mater Sci. Forum **264–268**, 461 (1998).
[24] J. A. Powell, L. G. Matus, and M. A. Kuczmarski, J. Electrochem. Soc. **134**, 1558 (1987).

[25] J. A. Powell, D. J. Larkin, L. G. Matus, W. J. Choyke, J. L. Bradshaw, L. Henderson, M. Yoganathan, J. Yang, and P. Pirouz, Appl. Phys. Lett. **56**, 1442 (1990).
[26] Cree Research, Inc., 2810 Meridian Parkway, Suite 176, Durham, NC 27713.
[27] J. A. Powell, D. J. Larkin, P. B. Abel, L. Zhou, and P. Pirouz, Inst. Phys. Conf. Ser. **142**, 77 (1996).
[28] J. A. Powell, D. J. Larkin, P. B. Abel, L. Zhou, and P. Pirouz, Transactions 3rd International High Temperature Electronics Conference, Albuquerque, NM, June 1996 (unpublished), p. II-3.
[29] D. J. Larkin, P. G. Neudeck, J. A. Powell, and L. G. Matus, Inst. Phys. Conf. Ser. **137**, 51 (1994).
[30] R. Schaub, G. Pensl, and M. Schulz, Appl. Phys. A: Solids Surf. **34**, 215 (1984).
[31] K. Hölzlein, G. Pensl, M. Schulz, and P. Stolz, Rev. Sci. Instrum. **57**, 1372 (1986).
[32] W. Keller, G. Pensl, and M. Schulz, Physica B **116**, 244 (1983).
[33] S. C. Sridhara, R. P. Devaty, and W. J. Choyke, J. Appl. Phys. (submitted).
[34] G. Wellenhofer and U. Rössler, Phys. Status Solidi B **202**, 107 (1997).
[35] V. N. Abakumov, V. I. Perel', and I. N. Yassievich, Sov. Phys. Semicond. **12**, 1 (1978) [Fiz. Tekh. Poluprovodn. **12**, 3 (1978)].
[36] B. K. Ridley, J. Phys. C **11**, 2323 (1978).
[37] L. Patrick, W. J. Choyke, and D. R. Hamilton, Phys. Rev. A **137**, 1515 (1965).
[38] L. L. Clemen, R. P. Devaty, M. F. MacMillan, M. Yoganathan, W. J. Choyke, D. J. Larkin, J. A. Powell, J. A. Edmond, and H. S. Kong, Appl. Phys. Lett. **62**, 2953 (1993).
[39] L. L. Clemen, R. P. Devaty, W. J. Choyke, J. A. Powell, D. J. Larkin, J. A. Edmond, and A. A. Burk, Jr., Inst. Phys. Conf. Ser. **137**, 297 (1994).
[40] A. Henry, C. Hallin, I. G. Ivanov, J. P. Bergman, O. Kordina, and E. Janzén, Inst. Phys. Conf. Ser. **142**, 381 (1996).
[41] A. Henry, C. Hallin, I. G. Ivanov, J. P. Bergman, O. Kordina, U. Lindefelt, and E. Janzén, Phys. Rev. B **53**, 13 503 (1996).
[42] T. L. Petrenko, A. A. Bugai, V. G. Baryakhtar, V. V. Teslenko, and V. D. Khavryutchenko, Semicond. Sci. Technol. **9**, 1849 (1994).
[43] T. L. Petrenko, V. V. Teslenko, A. A. Bugai, V. D. Khavryutchenko, and A. A. Klimov, Semicond. Sci. Technol. **11**, 1276 (1996).
[44] R. M. Potter, Mater. Res. Bull. **4**, S223 (1969).
[45] G. F. Kholuyanov, Sov. Phys. Solid State **6**, 2668 (1964) [Fiz. Tverd. Tela **6**, 3336 (1964)].
[46] W. Götz, A. Schöner, G. Pensl, W. Suttrop, W. J. Choyke, R. Stein, and S. Leibenzeder, J. Appl. Phys. **73**, 3332 (1993).
[47] P. J. Dean, ''Inter-impurity recombination in semiconductors,'' in *Progress in Solid State Chemistry* (Pergamon, New York, 1973), Vol. 8, pp. 1–126.
[48] D. G. Thomas, J. J. Hopfield, and W. M. Augustyniak, Phys. Rev. A **140**, 202 (1965).
[49] D. G. Thomas, M. Gershenzon, and F. A. Trumbore, Phys. Rev. A **133**, 269 (1964).
[50] K. Maeda, J. Phys. Chem. Solids **26**, 595 (1965).
[51] P. J. Dean and J. L. Merz, Phys. Rev. **178**, 1310 (1969).
[52] E. Zacks and A. Halperin, Phys. Rev. B **6**, 3072 (1972).
[53] W. J. Choyke, Mater. Res. Bull. **4**, S141 (1969).
[54] R. Z. Bachrach and O. G. Lorimor, Phys. Rev. B **7**, 700 (1973).
[55] D. M. Eagles, J. Phys. Chem. Solids **16**, 76 (1960).
[56] W. P. Dumke, Phys. Rev. **132**, 1948 (1963).
[57] H. B. Bebb, Phys. Rev. **185**, 1116 (1969).
[58] W. J. Choyke and Lyle Patrick, Phys. Rev. B **2**, 4959 (1970).